



On the composition of GRBs' Collapsar jets

Omer Bromberg,¹★ Jonathan Granot² and Tsvi Piran³

¹*Department of Astrophysical Sciences, Princeton University, 4 Ivy Lane, Princeton, NJ 08544, USA*

²*Department of Natural Sciences, The Open University of Israel, P.O.B 808, Ra'anana 43537, Israel*

³*Racah Institute of Physics, The Hebrew University, Jerusalem 91904, Israel*

Accepted 2015 January 30. Received 2015 January 27; in original form 2014 July 1

ABSTRACT

The duration distribution of long gamma-ray bursts (GRBs) reveals a plateau at durations shorter than ~ 20 s (in the observer frame) and a power-law decline at longer durations. Such a plateau arises naturally in the Collapsar model. In this model, the engine has to operate long enough to push the jet out of the stellar envelope and the observed duration of the burst is the difference between the engine's operation time and the jet breakout time. The jet breakout time inferred from the duration distribution (~ 10 s in the burst's frame) is comparable to the breakout time of both analytic estimates and numerical simulations (both 2D and 3D) of a hydrodynamic jet (~ 10 s for typical parameters). Recently, we have estimated analytically the breakout time of a Poynting-flux-dominated jet and have shown that it is consistent with 2D numerical simulations. We find that such a jet with the same overall energy breaks out much faster ($\lesssim 1$ s). If this result holds for 3D simulations it implies that only hydrodynamic jets are compatible with the duration of the plateau in the GRB duration distribution and hence the jet should be hydrodynamic during most of the time that its head is within the envelope of the progenitor star and around the time when it emerges from the star. This would naturally arise if the jet forms as a hydrodynamic jet in the first place or if it forms Poynting flux dominated but dissipates most of its magnetic energy early on within the progenitor star and emerges as a hydrodynamic jet.

Key words: hydrodynamics – MHD – methods: analytical – methods: statistical – gamma-ray burst: general – stars: Wolf-Rayet.

1 INTRODUCTION

Direct supernova–gamma-ray burst (SNe–GRB) observations as well as the location of long GRBs (LGRBs) within star-forming regions revealed that LGRBs arise during the death of massive stars (see e.g. Woosley & Bloom 2006, for a review). On the other hand, the observed spectral and temporal properties show that the prompt gamma-rays are emitted within relativistic jets at large distances ($\sim 10^{12}$ – 10^{16} cm) from the GRB progenitor (see e.g. Piran 2004, for a review). These observations are explained by the Collapsar model (MacFadyen & Woosley 1999). According to this model,¹ a compact object that forms at the centre of the collapsing star, launches a jet that drills a hole through the star. Once the jet breaks out from the stellar envelope it emits the observed gamma-rays far away from the progenitor star. While the Collapsar model success-

fully addresses the question of how a dying star produces a GRB, a major open question involves the nature of the relativistic jet. In this work, we address this question by examining the implications of recent understanding of the propagation of hydrodynamic (Bromberg et al. 2011, hereafter **BNPS11**) and MHD (Bromberg et al. 2014, hereafter **BGLP14**) jets within stellar envelopes.

Hydrodynamic jet propagation within stellar envelopes was studied both analytically (Mészáros & Waxman 2001; Matzner 2003; Lazzati & Begelman 2005; **BNPS11**) and numerically (MacFadyen & Woosley 1999; Aloy et al. 2000; MacFadyen, Woosley & Heger 2001; Zhang, Woosley & MacFadyen 2003; Lazzati & Begelman 2005; Morsony, Lazzati & Begelman 2007; Mizuta & Aloy 2009; Mizuta & Ioka 2013), while the propagation of a magnetic jet in stars was discussed in Proga et al. (2003), Uzdensky & MacFadyen (2007), Bucciantini et al. (2009), Levinson & Begelman (2013), **BGLP14** and Bromberg & Tekehovskoy (in preparation). These works show that as long as the jet does not breach out of the star it dissipates most of the energy that reaches its head. It follows that a minimal amount of energy is needed to push the jet out of the star. This translates to a minimal time, denoted the 'breakout time' t_b , that the engine must operate for a successful breakout of the jet. If

* E-mail: omerb@astro.princeton.edu

¹ We adopt here a broad definition of the Collapsar model, which involves any central engine that launches a jet within a collapsing star, regardless of the specific nature of the central engine or the composition of the jet.

the engine stops before this breakout time, the jet's head will not reach the stellar surface, and a regular GRB would not arise leading to a 'failed jet' or a 'failed GRB'.

A 'failed jet' might not go unnoticed. *Low-luminosity GRBs* (*lGRBs*) are a distinct group of GRBs characterized by their low (isotropic equivalent) luminosity, which is two orders of magnitude lower than the luminosity of typical GRBs, as well as by their low peak photon energy and their smooth, single-peaked light curves. Because of their low luminosity, *lGRBs* are detected only from nearby distances. Even though just a few *lGRBs* have been observed, their overall rate (per unit volume) is larger by about a factor of 10 than the overall rate of regular LGRBs (Cobb et al. 2006; Pian et al. 2006; Soderberg et al. 2006; Guetta & Della Valle 2007; Liang et al. 2007; Fan et al. 2011). There have been numerous arguments suggesting that *lGRBs* arise from 'failed jets' that do not break out from the stellar envelope (Kulkarni et al. 1998; MacFadyen et al. 2001; Tan, Matzner & McKee 2001; Campana et al. 2006; Wang et al. 2007; Waxman, Mészáros & Campana 2007; Katz, Budnik & Waxman 2010; Bromberg, Nakar & Piran 2011; Nakar & Sari 2012).

After the jet emerges from the stellar envelope it dissipates some of its energy at a large distance and produces the GRB. The overall behaviour of the prompt emission does not vary significantly during the burst (the second half of the prompt emission is rather similar to the first one). This suggests that the prompt emission arises at a more or less constant radius and not in a propagating single shell. This implies, in turn, that the GRB activity follows the central engine's activity (Sari & Piran 1997) and that the GRB will last as long as the central engine is active. Therefore, within the Collapsar model, the observed GRB duration (usually denoted by T_{90}) is the difference between the engine operation time, t_e , and the breakout time, t_b , namely $T_{90} = t_e - t_b$ (not accounting for the redshift). This leaves a distinctive mark on the duration distribution of Collapsars: if t_b is not negligible compared with the typical burst duration, the observed duration distribution of LGRBs will have a plateau at durations that are short compared to the typical t_b corrected for the typical redshift (Bromberg et al. 2012, 2013, hereafter **BNPS12**, **BNPS13**).

Such a plateau indeed appears in the duration distributions of LGRBs observed by all three major GRB satellites: *Swift*, BATSE and *Fermi*, with a typical duration of $t_b \sim 10\text{--}15$ s (**BNPS12**). This plateau may be interpreted in one of two ways. (1) It can be naturally explained within the Collapsar model, if a typical Collapsar jets spends $t_b \sim 10\text{--}15$ s within the star (**BNPS12**). Interestingly, this breakout time agrees well with the expected breakout time of hydrodynamic jets (**BNPS11**). (2) Alternatively such a distribution may reflect the intrinsic distribution of engine activity times, which, for some reason is flat up to ~ 10 . This last possibility requires of course a very short jet breakout time. While the Collapsar model predicts a plateau up to t_b , there is no available central engine model that predicts such an engine duration distribution. Thus, the first possibility is preferred and in the rest of the paper we adopt it and examine its implications.

While the observations are consistent with the expected breakout times of hydrodynamic jets, most current jet launching models are based, in one way or another, on a Poynting-flux-dominated outflow. In AGNs, this is the only viable option. While in GRBs thermally driven hydrodynamic jets (fireballs) are also possible, it is generally expected that those will be less powerful than the accompanying electromagnetic jets (e.g. Kawanaka, Piran & Krolik 2013). Motivated by these considerations, we (**BGLP14**) have recently investigated the propagation of a magnetic jet through a stellar envelope. Unlike hydrodynamic jets that typically cross the star at subrelativistic velocities, Poynting-flux-dominated jets have a narrower head and therefore encounter less resistance by the stel-

lar material and they cross the star at almost the speed of light. This results in a much shorter breakout time, which would lead to a different GRB duration distribution.

We consider here the implications of these recent findings on the type of jet that is expected to propagate in the star. We begin, in Section 2 with a brief review of the evidence for a plateau in the observed duration distribution of the different GRB satellites, updating the analysis to include the recent data from *Swift* and *Fermi*. In Section 3, we summarize the analytic results concerning the propagation of hydrodynamic and Poynting-flux-dominated jets. In Section 4, we examine the implications of the breakout time inferred from observations on nature of the jet. We consider the implications to three popular engines that may power the jet: a rapidly rotating accreting black hole (BH; Blandford & Znajek 1977), a BH accretion disc (Blandford & Payne 1982; Ustyugova et al. 2000) and a protomagnetar (Usov 1992; Metzger, Thompson & Quataert 2007). Our conclusions concerning the magnetization of Collapsar jets are summarized in Section 5, where we also mention possible caveats to these conclusions. Finally, we discuss the implications for the composition of the jets that emerge from the stellar envelope and produce the GRB.

2 OBSERVATIONS AND THE DURATION DISTRIBUTION OF COLLAPSARS

GRBs are traditionally divided into two groups, long and short. Following the original observations by BATSE (Kouveliotou et al. 1993), the dividing line in duration is usually placed at an observed duration, T_{90} , of 2 s. Naturally, there is an overlap between the two groups, especially at short durations (Nakar 2007; **BNPS13**). Although the high-energy properties of LGRBs and short GRBs (SGRBs) are rather similar, it was realized early on that the two groups have different progenitors. (i) The prompt high-energy spectrum of LGRBs is softer on average than that of SGRBs (e.g. Kouveliotou et al. 1993; Nakar 2007; **BNPS13**). We will use this feature in the following to distinguish between the two populations. (ii) The observed redshift distribution of SGRBs is different as was pointed out already in 1995 by Cohen & Piran (1995), using V/V_{\max} , and confirmed later by direct redshift observations (e.g. Berger 2010, 2013; Fong et al. 2013), with SGRBs typically at lower redshifts. (iii) Their environments are significantly different: LGRBs are observed exclusively in star-forming galaxies and are associated with the most active star-forming regions within these galaxies (Fruchter et al. 2006). SGRBs, on the other hand, are observed in a wide variety of galaxy types and within regions with different star formation rates (e.g. see reviews by Nakar 2007; Berger 2013). (iv) Finally, while some low-redshift LGRBs (and *lGRBs*) were observed associated with SNe, no SGRB was observed with such an association.

The distribution of GRB durations, dN_{GRB}/dT_{90} was studied by **BNPS12** and **BNPS13**, who showed that it is consistent with having a flat distribution of Collapsars at short durations. As the number of GRBs observed by *Swift* and *Fermi*-GBM has increased considerably, it is important to reexamine the significance of these results. We therefore reanalyze the data, following the same methodology of **BNPS12**, using the most recent data from these two satellites. Fig. 1 depicts the duration distribution, dN_{GRB}/dT_{90} , of BATSE²

² <http://gamma.mscf.nasa.gov/batse/grb/catalog/current/>, from 1991 April 21 to 2000 August 17.

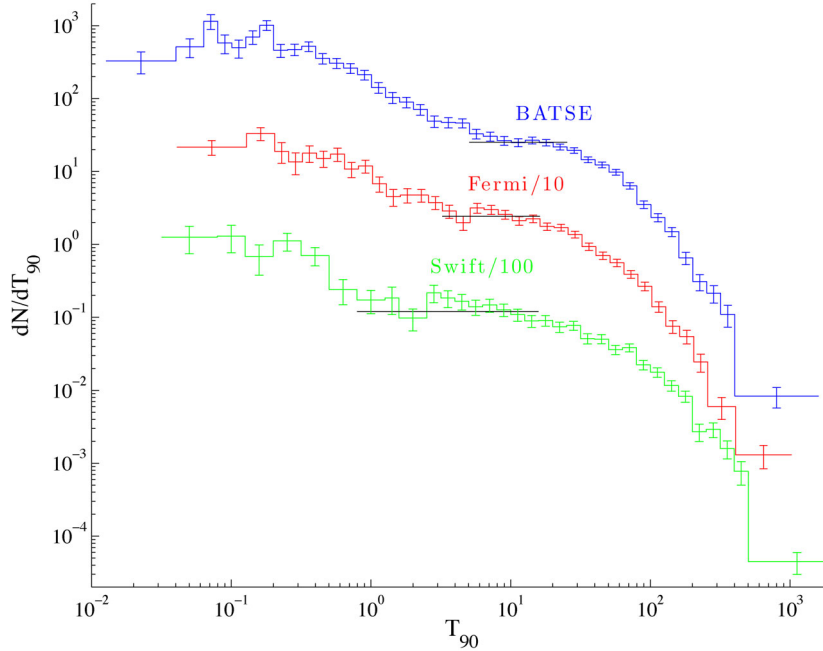


Figure 1. The duration distribution, dN_{GRB}/dT_{90} of BATSE (blue), *Fermi* (red) and *Swift* (Green) GRBs. The different curves are shifted so that they won't overlap each other. The data bins are evenly spaced in logarithmic scale with $\Delta \log(T_{90}) = 0.1$. Bins with less than 5 events are combined with their neighbour for statistics significance. The black horizontal lines mark the bins that fit a plateau at a confidence interval up to 2σ .

(2100 GRBs), *Fermi*-GBM³ (1310 GRBs) and *Swift*⁴ (800 GRBs). To fit a plateau in each data set we looked for the maximal number of bins that are consistent with a plateau at a confidence level ≤ 95 per cent (2σ).⁵ The best-fitting plateaus extend from 5 to 25 s in the BATSE data ($7.19/4 \chi^2/\text{DOF}$), from 2.5 to 17 s in the *Fermi*-GBM data ($10/5 \chi^2/\text{DOF}$) and from 1 to 20 s in the *Swift* data ($15.85/9 \chi^2/\text{DOF}$). We account for three free parameters in our fit: the height of the plateau and the two opposite ends of the plateau line. The differences between the maximal durations of the plateaus can be mostly attributed to the different sensitivity and triggering algorithms of the different detectors.

At short durations the plateau is concealed by the increasing number of non-Collapsar ('short') GRBs having a typical duration \lesssim a few seconds (BNPS13). As non-Collapsars have, on average, harder spectrum than Collapsars (e.g. Kouveliotou et al. 1993), we can reduce the relative number of non-Collapsars by choosing a hardness threshold (for each sample) and selecting only the events that are softer than this threshold. This should lead to a less prominent 'bump' at short duration. If the plateau is indeed an intrinsic property of the (softer) Collapsars duration distribution, it should extend to shorter durations in a softer subsample. To examine this effect, we select in each sample all the events that are softer than the median hardness of LGRBs ($T_{90} > 20$ s) in the sample (see BNPS13 for further details). Fig. 2 shows the duration distribution of the soft GRB subsamples. The plateaus indeed extend to much shorter durations than in the complete samples, supporting our hypothesis.

The best-fitting plateaus extend from 0.4 to 25 s in the BATSE data ($20.75/12 \chi^2/\text{DOF}$), from 0.4 to 17 s in the *Fermi*-GBM data ($8.7/10 \chi^2/\text{DOF}$) and from 0.2 to 20 s in the *Swift* data ($9.04/8 \chi^2/\text{DOF}$).

Taking a median redshift of $z \simeq 2$ for *Swift* GRBs and $z \simeq 1$ for *Fermi* and BATSE bursts we find that in the GRBs' cosmological frame these plateaus extend to 7–12 s, consistent with the results obtained by BNPS12. Note that the actual t_b may be somewhat longer than the duration that marks the end of the plateau, but it cannot be shorter. We use the duration interval of 7–12 s as our best estimate for the typical t_b .

It is important to stress that other distribution functions, which do not involve a plateau at short durations, have been used to fit the data. Specifically, a common way to fit the duration distribution is using two lognormal functions (Horváth 2002). However, unlike our case, these functions are arbitrary and are not based on a physical model. As such there is no particular reason to prefer one over the other. The existing plateau could appear in such a case due to some fine tuning in the matching of the two distributions (the collapsars and the NCs). However, since the distribution of Collapsars at short durations is no longer flat, maintaining the observed plateau when changing the hardness of the sample (see Fig. 2), and in particular its continual appearance when switching from one detector to another, requires extreme fine tuning. This is best demonstrated at [ftp://ftp.astro.princeton.edu/omerb/GRB_classification/](http://ftp.astro.princeton.edu/omerb/GRB_classification/), where we provide a movie describing how the BATSE duration distribution varies while we continuously soften the BATSE spectral window. The movie shows a fit of two lognormal functions to the data (NCs are marked in red, collapsars in green and the joint fit is shown in black). Note the required changes in both lognormal distributions.

Additional evidence that the Collapsar distribution remains constant at short duration arises from the indications that ≈ 30 per cent of *Swift* short bursts are Collapsars (Wanderman & Piran 2014). These findings pose a problem for any model whose low end of the collapsar duration distribution falls off significantly more steeply than flat (or a plateau). Specifically, they are inconsistent with a

³ <http://heasarc.gsfc.nasa.gov/W3Browse/fermi/fermigbrst.html>, from 2008 July 17 to 2014 February 14.

⁴ http://swift.gsfc.nasa.gov/archive/grb_table/, from 2004 December 17 to 2014 February 14.

⁵ The confidence level is defined here as $\int_0^{\chi^2} P(x, \nu) dx$, where $P(\chi^2, \nu)$ is the density function of χ^2 with ν degrees of freedom (Press et al. 1992).

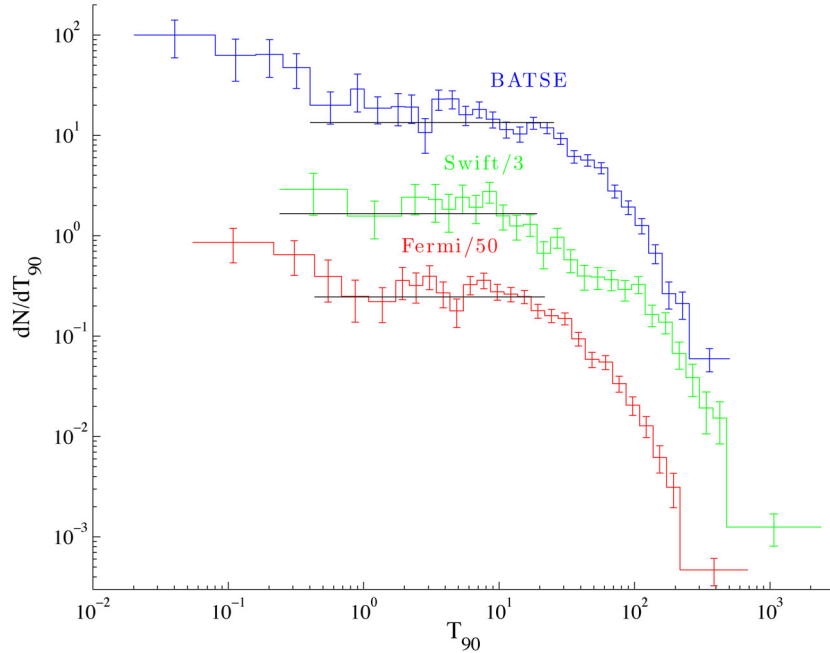


Figure 2. The duration distribution, dN_{GRB}/dT_{90} of the soft GRBs. The analysis is the same as in Fig. 1, only the data from each satellite contain only events that are softer than the median hardness of the LGRBs with durations $T_{90} > 20$ s. For the BATSE this corresponds to GRBs having a hardness ratio $HR_{32} < 2.6$. For *Fermi* the GRBs have a power-law spectral index < -1.5 and for *Swift* GRBs the spectral index < -1.7 . The analysis here updates the analysis in [BNPS13](#) using the newer data.

lognormal duration distribution for collapsars as this would result in too few short duration collapsars.

A second quantity that plays an important role in our analysis is the luminosity of the jet. The isotropic equivalent energy of LGRBs spans several orders of magnitudes in range, from $\sim 10^{49}$ erg to several times 10^{54} erg. The true energy, however, is more narrowly distributed. Bloom, Frail & Kulkarni (2003) estimated the real energy to be $\sim 1.33 \times 10^{51}$ erg, and a mean jet opening angle of $\theta_j \simeq 7^\circ$. Later works found this distribution to be wider, with a larger tail towards lower energies than towards higher energies. Taking a typical LGRB duration of ~ 30 s this energy corresponds to a typical one-sided jet luminosity of $L_j \sim 2 \times 10^{49}$ erg s^{-1} . Guetta, Piran & Waxman (2005) found similar values of typical jet luminosity and opening angle. Estimates of the true jet power show that a significant fraction of the jet power is emitted as gamma-rays, during the prompt phase (Panaitescu & Kumar 2001). [BNPS11](#) have shown that in a hydrodynamic jet the opening angle that is measured during the afterglow phase, is very close to the injection angle of the jet at the source (see however Mizuta & Ioka 2013 who claim that the injection angle is a few times larger than the observed one). In the following, we will use the observed L_j as a proxy for the true jet power during its propagation within the star adopting a canonical value of 2×10^{49} erg s^{-1} . For hydrodynamic jets we will use the opening angle of 7° as a canonical value for the injection angle. These jet properties correspond to an isotropic equivalence luminosity of $\sim 5 \times 10^{51}$ erg s^{-1} , consistent with the peak flux distribution found by Wanderman & Piran (2010).

3 THE BREAKOUT TIME OF A HYDRODYNAMIC AND A MAGNETIC JET

As long as the jet's head is within the star it pushes the stellar material in front of it, forming a bow shock ahead of the jet and a

cocoon of the shocked stellar material around it. The cocoon applies pressure on the jet and collimates it, thus changing its propagation velocity. The dynamics of this jet–cocoon system depends, among other things, on the magnetization of the jet. Unlike a hydrodynamic jet, a highly magnetized jet cannot effectively decelerate by shocks. Therefore, in order to match the speed of the shocked external medium at its head, it instead gradually decelerates by becoming narrower towards its head. This results in a head with a smaller cross-section, that propagates faster through the star than its hydrodynamic counterpart ([BGLP14](#)).

The jet's energy is dissipated at the head of the jet and flows into the cocoon. To continue propagating the head depends on the supply of fresh energy from the source. If the engine stops injecting energy, the head will essentially stop propagating once the information about the energy cutoff will reach it. The breakout time, t_b , is defined as the time of the engine shutoff for which the information about the shutoff reaches the jet's head when it is at the edge of the star. If the engine stops working at a time $t_e < t_b$, the head will 'feel' this while it is in the star and will stop propagating. In this case, the jet will not breakout and it will not produce a regular GRB.⁶ Since the information travels outwards at roughly the speed of light, the breakout time is related to the time at which the jet's head reaches the edges of the star as

$$t_b = \int_0^{R_*} \frac{dr}{\beta_h(r)c} - \frac{R_*}{c} \equiv \frac{R_*}{c} \frac{1 - \bar{\beta}_h}{\bar{\beta}_h}, \quad (1)$$

where $\beta_h(r)c$ is the instantaneous jet head velocity at r and $\bar{\beta}_h c$ is the average velocity.

Following [BNPS11](#) and [BGLP14](#), we obtain approximate analytic solutions to equation (1) for the non-relativistic and the

⁶ A failed jet produces, most likely, an *l*GRB when a shock wave generated by the dissipated energy breaks out from the stellar envelope.

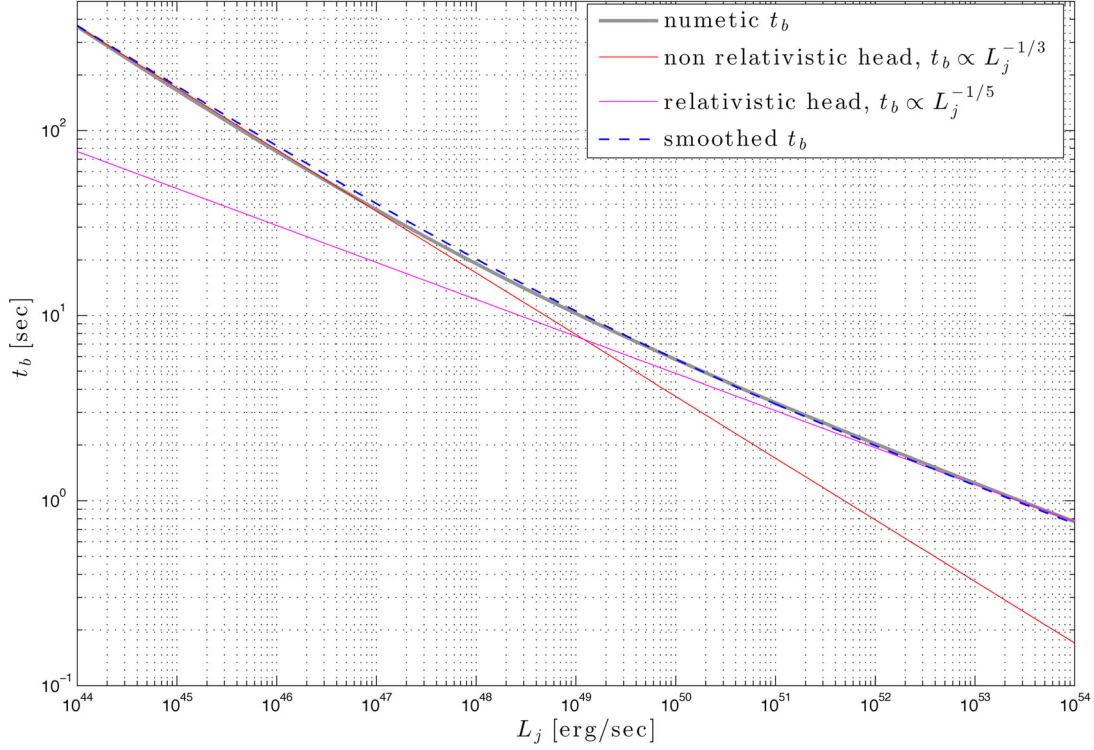


Figure 3. The breakout time, t_b , as a function of L_j calculated for a jet with an opening angle $\theta_j = 7^\circ$, and a star with a mass $M_* = 15 M_\odot$, radius $R_* = 4 R_\odot$ and a power-law density profile $\rho \propto r^{-2.5}$. The grey solid curve tracks the exact integration of equation (1), the red and magenta lines show the analytic approximation for the non-relativistic and the relativistic cases, respectively. The dashed blue line follows the smoothed analytic solution for t_b from equation (4).

relativistic limits. The former is characterized by $\Gamma_h \beta_h \ll 1$, where Γ_h is the corresponding Lorentz factor and in this limit $t_b \simeq R_* / \bar{\beta}_h c$. The latter is characterized by $\Gamma_h \beta_h \gg 1$ and in this case $t_b \simeq R_* / 2\Gamma_h^2 c$. The transition between the two limits occurs when $t_b \simeq R_* / c$, which according to equation (1) corresponds to $\bar{\beta}_h \simeq 1/2$. In the steep density profile of the stellar interior the jet's head, which is initially subrelativistic, accelerates. Therefore, if the jet becomes relativistic at some radius, R_{rel} , where $\Gamma_h \beta_h \simeq 1$, then it will remain so until it will break out.

For a hydrodynamic jet, t_b in the non-relativistic limit is obtained by integrating β_h using equation B3 in [BNPS11](#):

$$t_{\text{b,hyd}}^{\text{NR}} \simeq 37 L_{48}^{-1/3} R_{*,4R_\odot}^{2/3} M_{*,15M_\odot}^{1/3} \theta_{0.84}^{4/3} \left(\frac{3-\xi}{0.5} \right)^{7/15} \times \left(\frac{5-\xi}{2.5} \right)^{4/15} \text{ s.} \quad (2)$$

As canonical parameters we have used here a stellar mass of $M_* = 15 M_\odot$, a stellar radius $R_* = 4 R_\odot$ and we assume a power-law density profile: $\rho_* \propto r^{-\xi}$ with $\xi = 2.5$. Hereafter, we measure masses and radii in units of solar mass and solar radius, respectively, and use the subscript '*' to denote properties of the progenitor star. For all other quantities, we use the dimensionless form $A_x \equiv A/10^x$ measured in c.g.s units. In the relativistic limit, t_b is obtained by approximating $\beta_h \simeq 1 - 1/2\Gamma_h^2$, and using equation B14 from [BNPS11](#):

$$t_{\text{b,hyd}}^{\text{R}} \simeq 2 L_{52}^{-1/5} R_{*,4R_\odot}^{4/5} M_{*,15M_\odot}^{1/5} \theta_{0.84}^{4/5} \left(\frac{3-\xi}{0.5} \right)^{7/25} \times \left(\frac{5-\xi}{2.5} \right)^{4/25} \left(\frac{4.5}{7-\xi} \right) \text{ s.} \quad (3)$$

Fig. 3 depicts t_b as a function of L_j calculated with the fiducial values of injection angle and stellar properties. The grey line tracks the exact integration of equation (1). The solid red and magenta lines show the analytic approximations at the low-luminosity (non-relativistic) asymptote and at the high-luminosity (relativistic) asymptote, respectively. The transition between the asymptotes occurs at a luminosity range of about $10^{48} - 10^{51} \text{ erg s}^{-1}$ (for our chosen set of parameters), which is the range that is relevant for Collapsar jets. To obtain a useful analytic solution, we approximate the exact integration as (dashed blue line in Fig. 3):

$$t_{\text{b,hyd}} \simeq 6.5 R_{*,4R_\odot} \left[\left(\frac{L_j}{L_{\text{rel}}} \right)^{-2/3} + \left(\frac{L_j}{L_{\text{rel}}} \right)^{-2/5} \right]^{1/2}, \quad (4)$$

where L_{rel} is the transition luminosity between a non-relativistic breakout time and a relativistic one:

$$L_{\text{rel}} \simeq 1.6 \times 10^{49} R_{*,4R_\odot}^{-1} M_{*,15M_\odot} \theta_{0.84}^4 \left(\frac{3-\xi}{0.5} \right)^{7/5} \times \left(\frac{5-\xi}{2.5} \right)^{4/5} \left(\frac{7-\xi}{4.5} \right)^{15/2} \text{ erg s}^{-1}. \quad (5)$$

The corresponding breakout time is $t_b(L_{\text{rel}}) \simeq 9 R_{*,4R_\odot} \text{ s} \simeq R_* / c$, as expected. A typical Collapsar jet with luminosity of

$\sim 2 \times 10^{49}$ erg s⁻¹ and $\theta \sim 7^\circ$, is therefore at most mildly relativistic by the time it breaks out of the star.

A Poynting-flux-dominated jet becomes relativistic deep inside the star, even with a modest power (BGLP14):

$$\frac{R_{\text{rel}}}{R_*} \simeq 1.4 \times 10^{-2} \left[L_{49.3}^{-1} M_{*,15M_\odot} R_{*,4R_\odot}^{-3} r_{L,7}^2 \left(\frac{3-\xi}{0.5} \right) \right]^{1/\xi}. \quad (6)$$

This implies that here only the relativistic asymptotic solution is relevant. The corresponding breakout time is obtained, accordingly, using the relativistic approximation of β_h in BGLP14:

$$t_{\text{b,mag}} \simeq 0.8 L_{49.3}^{-1/3} M_{*,15M_\odot}^{1/3} r_{L,7}^{2/3} \left(\frac{0.5}{3-\xi} \right)^{2/3} \text{ s}. \quad (7)$$

This time is much shorter than the breakout time of a hydrodynamic jet with a similar luminosity.

4 IMPLICATIONS

The observed GRBs duration distribution indicates a typical breakout time of ~ 7 – 12 s. This time-scale arises naturally for hydrodynamic jets (equation 4) and it is much longer than typical breakout times of Poynting-flux-dominated jets (equation 7). For the canonical hydrodynamic jet used in this work these breakout times imply a stellar radius of $R_* \simeq (3M_{*,15M_\odot}^{-1/2} - 6M_{*,15M_\odot}^{-1/4}) R_\odot$, which is consistent with expected radii of Wolf–Rayet stars that are the likely progenitors of LGRBs. The different power-law indices in the mass arise from the fact that for $3R_\odot$ the jet's head is non-relativistic ($L_{\text{rel}} < L_j$) while for $6R_\odot$ it is relativistic ($L_j > L_{\text{rel}}$, see equation 4).

For a Poynting dominated jet, these breakout times could arise only if the light cylinder radius $r_L \sim (2.5\text{--}5) \times 10^8$ cm (equation 7). This value is larger than the one that expected for GRBs central engines, thus disfavouring this option. Before ruling out Poynting-flux-dominated jets we turn to examine three central engine models and explore whether such a large value of the light cylinder is a viable option. Clearly, unlike the general discussion we had so far, this discussion is model dependent, as assumptions have to be made on the specific nature of the central engine and the jet acceleration mechanism. Still it gives a good indication on the question of whether a central engine producing such a Poynting-flux-dominated jet is plausible.

A light cylinder radius, $r_L \sim (2.5\text{--}5) \times 10^8$ cm, corresponds to an angular frequency of the magnetosphere at the base of the jet of $\Omega_m = c/r_L \simeq 60\text{--}120$ rad s⁻¹. It is generally accepted that the Poynting dominated jet is driven by the rotation of the central engine. The field lines that are connected to the rotating central object are wound up by the rotation, generating a toroidal field. The toroidal ‘hoops’ then propagate outward under their own pressure and transfer most of the energy outwards in the form of Poynting flux. Therefore, the implied value of Ω_m has a direct consequence on the rotation and on the luminosity that can be generated by the central object. We consider the implications on three objects that have been suggested to power a Poynting dominated jet: An accreting, rotating BH (e.g. Blandford & Znajek 1977), a magnetized accretion disc (e.g. Blandford & Payne 1982; Ustyugova et al. 2000; Lovelace et al. 2002) and a rapidly rotating magnetar (Usov 1992; Metzger et al. 2007).

In an accreting rotating BH, the magnetic field lines of the jet thread the horizon of the BH. The horizon has an effective resistance of $4\pi/c$, which produces a drag on the field lines and causes them to rotate at $\Omega_m \simeq \eta\Omega_H$, where Ω_H is the angular velocity of the BH

and η is usually estimated as $1/2$ (e.g. Blandford & Znajek 1977). The BH's angular velocity satisfies $\Omega_H = ac/R_H$, where a is the dimensionless spin of the BH and $R_H = GM_H(1 + \sqrt{1-a^2})/c^2$ is the radius of the horizon giving

$$\frac{a}{1 + \sqrt{1-a^2}} \simeq 5 \times 10^{-3} \left(\frac{\eta}{0.5} \right)^{-1} \Omega_{m,2} M_{H,5M_\odot}. \quad (8)$$

The limit $\Omega_m \simeq 60\text{--}120$ rad s⁻¹ implies a very low value of $a \approx (3\text{--}6) \times 10^{-3}$. The corresponding power output that goes into to each jet is (Blandford & Znajek 1977)

$$L_j \simeq 5.5 \times 10^{49} B_{16}^2 M_{5M_\odot}^2 \left(\frac{a + a\sqrt{1-a^2}}{0.02} \right)^2 \text{ erg s}^{-1}. \quad (9)$$

Thus, the slow rotating BH can provide the observed luminosity of LGRBs, if the magnetic field on the horizon is about $\sim 10^{16}$ G. Such a high magnetic field requires an efficient amplification process either in an accretion disc or in the core, prior to its collapse, and is likely accompanied by a significant rotation. It is hard to imagine how the BH can acquire such a high magnetic field without being spun up by the angular momentum of the accreted matter, making this scenario less realistic.

The jet might be launched from the accretion disc itself. A magnetized accretion disc rotates differentially around the BH. Magnetic field lines that are connected to the disc at different radii rotate at different angular velocities and have different light cylinder radii. Therefore, if the jet is powered by the accretion disc, the constraint on Ω_m of the jet implies a constraint on the disc's radius where most of the jet's energy is injected. Assuming a Keplerian (and for simplicity Newtonian) disc, this radius is $\simeq 50 r_g \Omega_{m,2}^{-2/3} M_{H,5M_\odot}^{-2/3}$, where $r_g = GM_H/c^2$ is the gravitational radius of the BH. Such an injection radius seems too large for realistic engine disc models. For example, Lovelace et al. (2002) and Lovelace & Romanova (2003) found that a Keplerian disc around a Schwarzschild BH radiates almost all of its Poynting flux inside its last stable orbit radius, located at $\sim 6r_g$. Note that a coupling in the radial direction between different parts of the disc will only increase the rotational velocity at each radius and will further increase the radius corresponding to a given Ω_m .

In a third scenario, the jet is powered by a rapidly rotating magnetar. In this case, the magnetic field lines are anchored to the surface of the neutronstar and corotate with it. Therefore, the bounds we infer for Ω_m determine the rotational velocity of the magnetar. The power that goes into the jet can be evaluated by integrating the Poynting flux, $\frac{c}{4\pi} \mathbf{E} \times \mathbf{B}$, across the field lines that are associated with the jet. The power is maximized when we assume that all the field lines are channelled into the jet and the magnetosphere has the topology of a split monopole near the base of the magnetar. Such a topology is expected, at least in the early stages of the magnetar, when the magnetosphere is still baryon loaded by the neutrino-driven wind blowing from the surface of the magnetar (Usov 1992; Metzger et al. 2007). This gives a one-sided jet power of

$$\dot{E} \simeq 10^{49} B_{16}^2 R_6^4 \Omega_2^2 \text{ erg s}^{-1}, \quad (10)$$

where B is the magnetic field at the surface of the magnetar. A configuration of a force-free magnetosphere will give an even lower luminosity than that (Spitkovsky 2006). It can be seen that a typical power of LGRB jets can barely be satisfied with the inferred rotational velocity, even in the extreme condition where all magnetic field lines are open, and only if $B \sim 10^{16} R_6^{-2}$ G. Note that Dall'Osso, Granot & Piran (2012) suggest that even though magnetars are born with such internal fields, their initial dipole field

that is relevant here is $\lesssim 10^{15}$ G. Like in the case of the BH it is hard to see how such high field can be obtained without requiring a significant rotation of the magnetar. Moreover, estimates of the rotational energy of the magnetar, assuming it rotates rigidly, give

$$E_{\text{rot}} \approx 5 \times 10^{48} \Omega_2^2 R_6^2 M_{1.4 M_\odot}, \quad (11)$$

where R and M are the radius and mass of the magnetar. This rotational energy is about two orders of magnitude lower than the energy of a typical LGRB. Thus the magnetar scenario is also rejected.

We find that in all three central engine models that we considered: an accreting BH, a BH accretion disc or a rapidly rotating magnetar, are incompatible with a large r_L that is required to produce the breakout times of 7–12 s, inferred from the duration distribution. This implies that the jet must be launched hydrodynamically or alternatively if the jet is launched Poynting flux dominated it should dissipate its magnetic energy rapidly within the star and become hydrodynamic. In either case the jet emerging from the stellar envelope is not Poynting flux dominated.

5 CONCLUSIONS

The lack of a strong evolution in the properties of the prompt emission of LGRBs suggests that the conditions within the emission regions are rather constant in time. A single moving shell would have expanded by a factor of ~ 10 – 100 during the duration of a burst and it is unlikely to maintain constant conditions as it emits the prompt gamma-ray emission over such a wide range of radii. This, in turn, suggests that the duration of the burst is determined by the activity of the central engine and not by a local process within the emission region. In a Collapsar model in which the jet has to breakout from the progenitor star, we therefore expect that $T_{90} = t_e - t_b$. This relation implies a plateau in the duration distribution of GRBs at durations shorter than the typical breakout time. Indeed, such a plateau exists in the duration distribution of the three major GRB satellites, *Swift*, *Fermi* and BATSE at durations shorter than ~ 25 s (BNPS12), confirming the basic assertions of this model. Reanalysis of the latest *Swift* and *Fermi* data confirms the presence of this plateau up to observed durations of ~ 17 – 25 s, which correspond to a breakout time $t_b \sim 7$ – 12 s in the source frame.

The inferred breakout time is consistent with the propagation time of a hydrodynamic jet, and it implies a progenitor radius of $\sim (3$ – $6) R_\odot$. On the other hand, this breakout time is too long for typical parameters expected for a Poynting dominated jet. A breakout time of ~ 7 – 12 s requires a light cylinder radius of $r_L \simeq (2.5$ – $5) \times 10^8$ cm, corresponding to an angular frequency of $\Omega_m \simeq 60$ – 120 rad s^{-1} at the base of the jet.

Such a large value of r_L and the corresponding low Ω_m are inconsistent with the three most popular Poynting flux jet acceleration models. If the jet is powered by an accreting BH, this angular frequency implies a very low spin parameter of the BH, $a \lesssim 0.01$. This value is most likely too low to allow an amplification of the magnetic field to $\sim 10^{16}$ G, required to power the GRB jet. Similarly, the low Ω_m renders magnetars as an unlikely sources. The magnetar would simply rotate too slow to supply the observed power and the total energy. Finally, an accretion disc is unlikely to power the jet as well, since the low rotation rate implies that it should inject most of the energy at a distance of about 50 gravitational radii, too far for reasonable disc engine models.

We conclude that during most of its propagation within the star the jet has a low magnetization and it propagates as a hydrodynamic jet.

This result leads to some interesting implications on the properties of LGRB internal engines and the conditions at the base of the jets. One possibility is that the jet is launched hydrodynamically at the source. The most probable process for that is neutrino annihilation above the rotational axis of the central engine (e.g. Eichler et al. 1989; Levinson & Eichler 1993). This scenario can work only if the accretion rate is $\gtrsim 0.1 M_\odot s^{-1}$, so that neutrino emission is large enough to power the observed jets (Kawanaka et al. 2013; Levinson & Globus 2013). The high accretion rate must be sustained throughout the entire duration of the GRB which can last from tens to hundreds of seconds. Though a duration of $\lesssim 30$ s seems to be consistent with such a model (e.g. Lindner et al. 2010), it seems unlikely to be capable of powering longer duration GRBs.

A second possibility is that the jet is launched Poynting dominated but it dissipates most of its magnetic energy close to the source, and it then propagates as a hydrodynamic jet. An appealing process for such efficient dissipation is the kink instability (Lyubarskij 1992; Eichler 1993; Spruit, Foglizzo & Stehle 1997; Begelman 1998; Lyubarskii 1999; Giannios & Spruit 2006). However, we (BGLP14) have shown that Collapsar jets are unlikely to be disrupted by the kink instability. Thus, the dissipation should arise from a different process.

A third possibility is that the jet changes its character with time. Our conclusion concerning the jet composition applies only to the initial phase, while its head is still within the stellar envelope. This phase, which lasts about 10 s, must be predominantly hydrodynamic. Once the jet has breached out of the star, it could be Poynting flux dominated. This would require, of course, a more complicated central engine that switches from one mode to another. While this seems contrived, remarkably, some magnetar models suggest such a possibility (Metzger et al. 2011). One can also imagine accretion disc models that initially cool via neutrinos and later on as the accretion rate decreases, becomes Poynting flux dominated (Kawanaka et al. 2013). However, all such models require some degree of coincidence as the central engine does not receive any feedback from the propagating jet and there is no a priori reason that the transition from one composition to the other would take place just at the right stage.

Before concluding we note that our interpretation of the observed temporal duration distribution depends on the condition $T_{90} = t_e - t_b$. This condition holds if the prompt gamma-ray activity follows the activity of the central engine and if the jet has to penetrate the envelope of the collapsing star. The first assumption is supported by observational features of the prompt GRBs. The second one is the central assumption of any Collapsar model. With both assumptions and with $t_b \sim 10$ s the plateau and the break in the duration distribution arise naturally for Collapsars with hydrodynamic jets. If one assumes that T_{90} is not determined by the central engine or if one asserts that $t_b \ll 10$ s (in which case the plateau does not reflect the jet breakout time), one has to suggest a model for the GRB duration distribution that explains the observed plateau at short durations and the break at ~ 10 s, as well as other temporal properties of LGRBs. We are not aware of such a model.

We conclude that, provided that (i) the plateau in the collapsar distribution indeed arises from a jet breakout and not as a result of a yet unknown feature of the central engine, and (ii) that the results of BGLP14 concerning the short breakout time of a Poynting-flux-dominated jet hold, then the jets that emerge from the progenitor envelopes are not Poynting flux dominated. It is interesting to note that our results are consistent with the recent findings of Beniamini & Piran (2014) or Beloborodov (2013). These authors have shown, the first quite generally and the second specifically for photospheric

models that, based on the properties of the observed spectra, it is unlikely that within the emitting region of the prompt gamma-rays, the ratio of magnetic to total energy density is large. While these studies explore different regimes: the stellar envelope in our case and the emitting regions for those other studies, both reach the same conclusion concerning the jet's composition at large distances from the central engine.

ACKNOWLEDGEMENTS

We thank E. Nakar, A. Philippov, A. Tchekhoskoy and the anonymous referee for meaningful discussions. This research was supported by the ERC advanced research grant 'GRBs' by the I-CORE (grant no. 1829/12) and by HUJ-USP grant and by a grant from the Israel space agency, SELA.

REFERENCES

- Aloy M. A., Müller E., Ibáñez J. M., Martí J. M., MacFadyen A., 2000, *ApJ*, 531, L119
- Begelman M. C., 1998, *ApJ*, 493, 291
- Beloborodov A. M., 2013, *ApJ*, 764, 157
- Beniamini P., Piran T., 2014, *MNRAS*, 445, 3892
- Berger E., 2010, *ApJ*, 722, 1946
- Berger E., 2013, *ARA&A*, 52, 43
- Blandford R. D., Payne D. G., 1982, *MNRAS*, 199, 883
- Blandford R. D., Znajek R. L., 1977, *MNRAS*, 179, 433
- Bloom J. S., Frail D. A., Kulkarni S. R., 2003, *ApJ*, 594, 674
- Bromberg O., Nakar E., Piran T., 2011, *ApJ*, 739, L55
- Bromberg O., Nakar E., Piran T., Sari R., 2011, *ApJ*, 740, 100 (BNPS11)
- Bromberg O., Nakar E., Piran T., Sari R., 2012, *ApJ*, 749, 110 (BNPS12)
- Bromberg O., Nakar E., Piran T., Sari R., 2013, *ApJ*, 764, 179 (BNPS13)
- Bromberg O., Granot J., Lyubarsky Y., Piran T., 2014, *MNRAS*, 443, 1532 (BGLP14)
- Bucciantini N., Quataert E., Metzger B. D., Thompson T. A., Arons J., Del Zanna L., 2009, *MNRAS*, 396, 2038
- Campana S. et al., 2006, *Nature*, 442, 1008
- Cobb B. E., Bailyn C. D., van Dokkum P. G., Natarajan P., 2006, *ApJ*, 645, L113
- Cohen E., Piran T., 1995, *ApJ*, 444, L25
- Dall'Osso S., Granot J., Piran T., 2012, *MNRAS*, 422, 2878
- Eichler D., 1993, *ApJ*, 419, 111
- Eichler D., Livio M., Piran T., Schramm D. N., 1989, *Nature*, 340, 126
- Fan Y.-Z., Zhang B.-B., Xu D., Liang E.-W., Zhang B., 2011, *ApJ*, 726, 32
- Fong W. et al., 2013, *ApJ*, 769, 56
- Fruchter A. S. et al., 2006, *Nature*, 441, 463
- Giannios D., Spruit H. C., 2006, *A&A*, 450, 887
- Guetta D., Della Valle M., 2007, *ApJ*, 657, L73
- Guetta D., Piran T., Waxman E., 2005, *ApJ*, 619, 412
- Horváth I., 2002, *A&A*, 392, 791
- Katz B., Budnik R., Waxman E., 2010, *ApJ*, 716, 781
- Kawanaka N., Piran T., Krolik J. H., 2013, *ApJ*, 766, 31
- Kouveliotou C., Meegan C. A., Fishman G. J., Bhat N. P., Briggs M. S., Koshut T. M., Paciesas W. S., Pendleton G. N., 1993, *ApJ*, 413, L101
- Kulkarni S. R. et al., 1998, *Nature*, 395, 663
- Lazzati D., Begelman M. C., 2005, *ApJ*, 629, 903
- Levinson A., Begelman M. C., 2013, *ApJ*, 764, 148
- Levinson A., Eichler D., 1993, *ApJ*, 418, 386
- Levinson A., Globus N., 2013, *ApJ*, 770, 159
- Liang E., Zhang B., Virgili F., Dai Z. G., 2007, *ApJ*, 662, 1111
- Lindner C. C., Milosavljević M., Couch S. M., Kumar P., 2010, *ApJ*, 713, 800
- Lovelace R. V. E., Romanova M. M., 2003, *ApJ*, 596, L159
- Lovelace R. V. E., Li H., Koldoba A. V., Ustyugova G. V., Romanova M. M., 2002, *ApJ*, 572, 445
- Lyubarskii Y. E., 1999, *MNRAS*, 308, 1006
- Lyubarskij Y. E., 1992, *Sov. Astron. Lett.*, 18, 356
- MacFadyen A. I., Woosley S. E., 1999, *ApJ*, 524, 262
- MacFadyen A. I., Woosley S. E., Heger A., 2001, *ApJ*, 550, 410
- Matzner C. D., 2003, *MNRAS*, 345, 575
- Mészáros P., Waxman E., 2001, *Phys. Rev. Lett.*, 87, 171102
- Metzger B. D., Thompson T. A., Quataert E., 2007, *ApJ*, 659, 561
- Metzger B. D., Giannios D., Thompson T. A., Bucciantini N., Quataert E., 2011, *MNRAS*, 413, 2031
- Mizuta A., Aloy M. A., 2009, *ApJ*, 699, 1261
- Mizuta A., Ioka K., 2013, *ApJ*, 777, 162
- Morsony B. J., Lazzati D., Begelman M. C., 2007, *ApJ*, 665, 569
- Nakar E., 2007, *Phys. Rep.*, 442, 166
- Nakar E., Sari R., 2012, *ApJ*, 747, 88
- Panaitescu A., Kumar P., 2001, *ApJ*, 560, L49
- Pian E. et al., 2006, *Nature*, 442, 1011
- Piran T., 2004, *Rev. Mod. Phys.*, 76, 1143
- Press W. H., Teukolsky S. A., Vetterling W. T., Flannery B. P., 1992, *Numerical Recipes in C. The Art of Scientific Computing*. Cambridge Univ. Press, Cambridge
- Proga D., MacFadyen A. I., Armitage P. J., Begelman M. C., 2003, *ApJ*, 599, L5
- Sari R., Piran T., 1997, *ApJ*, 485, 270
- Soderberg A. M. et al., 2006, *Nature*, 442, 1014
- Spitkovsky A., 2006, *ApJ*, 648, L51
- Spruit H. C., Foglizzo T., Stehle R., 1997, *MNRAS*, 288, 333
- Tan J. C., Matzner C. D., McKee C. F., 2001, *ApJ*, 551, 946
- Usov V. V., 1992, *Nature*, 357, 472
- Ustyugova G. V., Lovelace R. V. E., Romanova M. M., Li H., Colgate S. A., 2000, *ApJ*, 541, L21
- Uzdensky D. A., MacFadyen A. I., 2007, *Phys. Plasma*, 14, 056506
- Wanderman D., Piran T., 2010, *MNRAS*, 406, 1944
- Wanderman D., Piran T., 2014, preprint ([arXiv:1405.5878](https://arxiv.org/abs/1405.5878))
- Wang X.-Y., Li Z., Waxman E., Mészáros P., 2007, *ApJ*, 664, 1026
- Waxman E., Mészáros P., Campana S., 2007, *ApJ*, 667, 351
- Woosley S. E., Bloom J. S., 2006, *ARA&A*, 44, 507
- Zhang W., Woosley S. E., MacFadyen A. I., 2003, *ApJ*, 586, 356

This paper has been typeset from a $\text{\TeX}/\text{\LaTeX}$ file prepared by the author.